Progress In Electromagnetics Research C, Vol. 53, 67–73, 2014

Compact Wideband Differential Bandpass Filter Using a Marchand Balun

Shi Bai[1], Wenjie Feng[2, *], and Wenquan Che[2]

Abstract—A novel compact wideband differential bandpass filter with wideband common mode suppression using a Marchand balun is presented in this paper. Open/shorted coupled lines and stubs are used to improve the selectivity for the differential mode and common mode suppression. The demonstrated filter with a compact size of 50 mm × 30 mm exhibits a fractional bandwidth of 53% centered at 3.0 GHz and 13 dB common-mode suppression from 0 to 9 GHz. The theoretical and measured results agree well with each other and show good in-band performances.

1. INTRODUCTION

Compact wideband differential filters with simple structures, wideband common mode rejection capability are highly needed in modern wireless communication systems [1]. In the past few years, many approaches have been demonstrated for single band, dual-band and wideband differential filters [2–15]. For the wideband differential filters [8–15], two kinds of wideband microstrip differential filters with good common-mode suppression in the passband are proposed in [8, 9], but the suppression of the common-mode signals is not good in out-of-band. In [10, 11], using the 180° phase inverters, some differential ultra-wideband (UWB) balanced bandpass filters based on double-sided parallel-strip line (DSPSL) are illustrated. However, the upper stopbands for the differential mode are a little narrow. In addition, microstrip-to-slotline transition and transversal signal-interference concepts are also introduced to realize UWB differential bandpass filters in [12, 13]. However, the selectivity and upper stopband for the differential mode need to be further improved. In [14, 15], several wideband differential bandpass filters based on T-shaped structures with wideband common mode suppression are introduced, but low characteristic impedance of the stub for the T-shaped structure increase the loss for the differential mode and the circuit size need to be further reduced.

In this paper, a novel microstrip wideband differential filter using only a Marchand balun is proposed. Two stepped impedance resonators (SIRs) are used to improve the selectivity for the differential mode and common mode suppression. The bandwidth for the differential mode can be adjusted easily by changing the coupling coefficient of open/shorted coupled lines, wideband common mode suppression can be also realized by the all stopband transmission characteristic of the coupling circuit. A prototype of the differential filter operating at 3.0 GHz is constructed on the dielectric substrate with $\varepsilon_r = 2.65$, $h = 0.5$ mm, and $\tan\delta = 0.003$.

2. ANALYSIS OF PROPOSED WIDEBAND DIFFERENTIAL FILTER

Figure 1(a) shows the the circuit of the wideband differential filter, from port 1 ($1'$) to ports 2, $2'$, two open/shorted coupled lines (Z_{oe} Z_{oo}, θ) are located symmetrically, the electrical length of shorted/open stubs paralleled in port 1, $1'$ and 2, $2'$ are all θ. The characteristic impedances of the microstrip lines

Received 24 July 2014, Accepted 16 August 2014, Scheduled 25 August 2014

* Corresponding author: Wenjie Feng (fengwenjie1985@163.com).

[1] School of Information Science and Engineering, Southeast University, Nanjing 210096, China. [2] Department of Communication Engineering, Nanjing University of Science & Technology, Nanjing 210094, China.

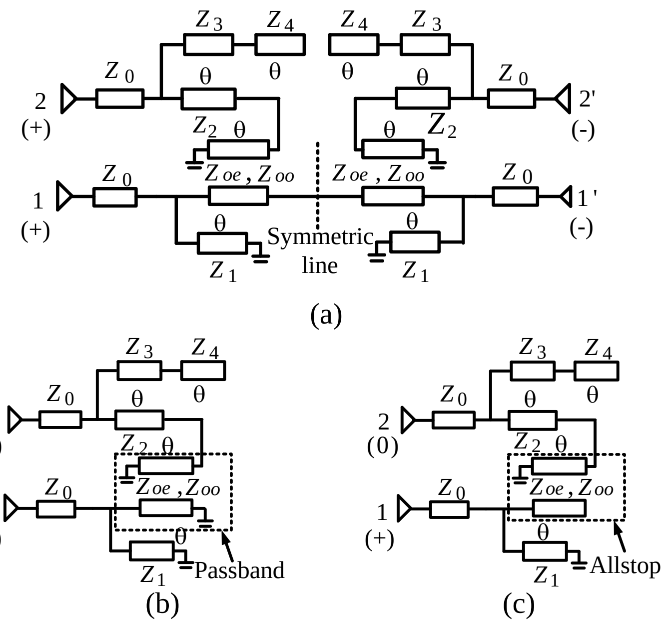

Figure 1. Circuits of proposed wideband differential filter. (a) Equivalent circuit of the wideband differential filter. (b) Differential mode circuit. (c) Common mode circuit.

at the input/output ports are $Z = 50\,\Omega$. The equivalent half circuits of the differential/common-mode can be used for theoretical analysis conveniently [1], as shown in Figures 1(b) and (c).

To realize good impedance matching for each port, the input impedance ($Z_{in} = Z_0$) and output impedance ($Z_{out} = Z_0$) of the Marchand balun should meet the following conditions [16]

$$k = (Z_{oe} - Z_{oo})/(Z_{oe} + Z_{oo}) = 1/\sqrt{1 + 2Z_2/Z_0} \tag{1}$$

For a given set of balun impedances, the coupled line parameters (Z_{oe}, Z_{oo}) are not unique, and the bandwidth for the Marchand balun increases as the coupling coefficient k increases [16]. In addition, the quarter-wavelength transmission line (Z_2, θ) can be seen as an impedance transformer, and the input impedance of the shorted coupled lines is [16]

$$Z_{short} = 2Z_{oe}Z_{oo}/(Z_{oe} - Z_{oo}) \tag{2}$$

and

$$Z_2 = \sqrt{Z_o \times Z_{short}} \tag{3}$$

From the Equations (1)–(3), we can get the following relationships:

$$Z_{oe} = \frac{Z_2^2/\sqrt{Z_0(Z_0 + 2Z_2)}}{1 - (1/\sqrt{1 + 2Z_2/Z_0})}, \quad Z_{oo} = \frac{Z_2^2/\sqrt{Z_0(Z_0 + 2Z_2)}}{1 + (1/\sqrt{1 + 2Z_2/Z_0})} \tag{4}$$

Referring to the Equations (1)–(4), the desired relationship between Z_{oe} and Z_{oo} for different combinations of the Z_2 is plotted in Figure 2. For a given set of characteristic impedance of Z_2, the coupled line parameters (Z_{oe} and Z_{oo}) are unique, and the coupling coefficient k decreases as Z_2 increases. In this way, by proper choosing the even/odd-mode characteristic impedance of the open/shorted coupled line and the characteristic impedance of Z_2, good impedance matching can be realized for each port of Figure 1(a).

In addition, when Z_1, Z_2, Z_{oe}, and Z_{oo} are fixed, the input admittance of the stepped impedance resonators Y_{SIR} is

$$Y_{\mathrm{SIR}} = jY_3\left(Z_3 \tan\theta + Z_4 \tan\theta\right) / \left(Z_4 - Z_3 \tan^2\theta\right) \tag{5}$$

When $Y_{\mathrm{SIR}} \to \infty$, the transmission zeros near the passband of the differential mode can be acquired

$$\theta_{tz1} = \arctan\sqrt{Z_4/Z_3}, \quad \theta_{tz2} = \pi - \arctan\sqrt{Z_4/Z_3} \tag{6}$$

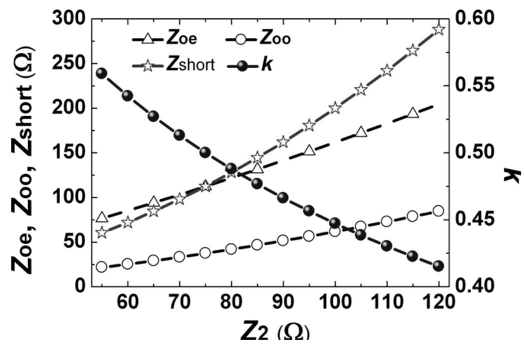

Figure 2. Relationship between Z_{oe} and Z_{oo} in case of Z_2, $Z_0 = 50\,\Omega$.

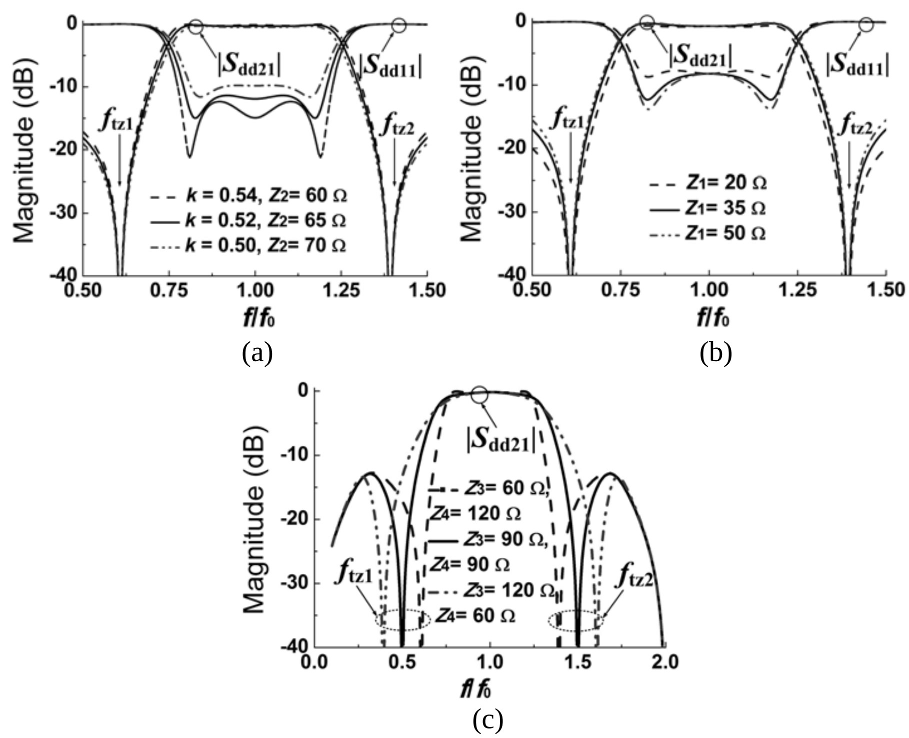

Figure 3. Simulated results of the differential mode for the proposed wideband differential filter. (a) $|S_{dd21}|$ and $|S_{dd11}|$ versus Z_2 and k, $Z_1 = 30\,\Omega$, $Z_3 = 60\,\Omega$, $Z_4 = 120\,\Omega$. (b) $|S_{dd21}|$ and $|S_{dd11}|$ versus Z_1 and Z_4, $Z_1 = 30\,\Omega$, $Z_3 = 60\,\Omega$, $Z_4 = 120\,\Omega$, $Z_{oe} = 103.2\,\Omega$, $Z_{oo} = 63.2\ \Omega$. (c) $|S_{dd21}|$ versus Z_3 and Z_4, $Z_1 = 30\,\Omega$, $Z_{oe} = 103.2\,\Omega$, $Z_{oo} = 63.2\,\Omega$.

Figures 3(a)–(c) show the simulated results of the differential mode versus characteristic impedance Z_1, Z_3, Z_4, Z_{oe} and Z_{oo}. The bandwidth of the differential mode increases as coupling coefficient k ($k = (Z_{oe} - Z_{oo})/(Z_{oe} + Z_{oo})$) increases, and decreases as Z_1 decreases. As a matter of fact, when the characteristic impedance Z_1 of the shorted stub becomes smaller, the capacitance of the shorted stub increases while the inductance decreases, and the shorted stub can be seen as an ideal lossless parallel resonance circuit in the center frequency f_0. Because the Q factor of the passband for the shorted stub is proportional to the susceptance slope parameter $\sqrt{C_S/L_S}$, when the Q factor increases, the bandwidth for the passband will become narrower [16]. For the common mode circuit of Figure 1(c), the open/shorted coupled lines are all bandstop structures [16], and it is very easy to realize a wideband common mode suppression in/out-of-band of the differential mode. The simulated results of Figure 1(c) versus Z_1, Z_3, Z_4, Z_{oe} and Z_{oo} are shown in Figures 4(a)–(c). Due to the two introduced stepped

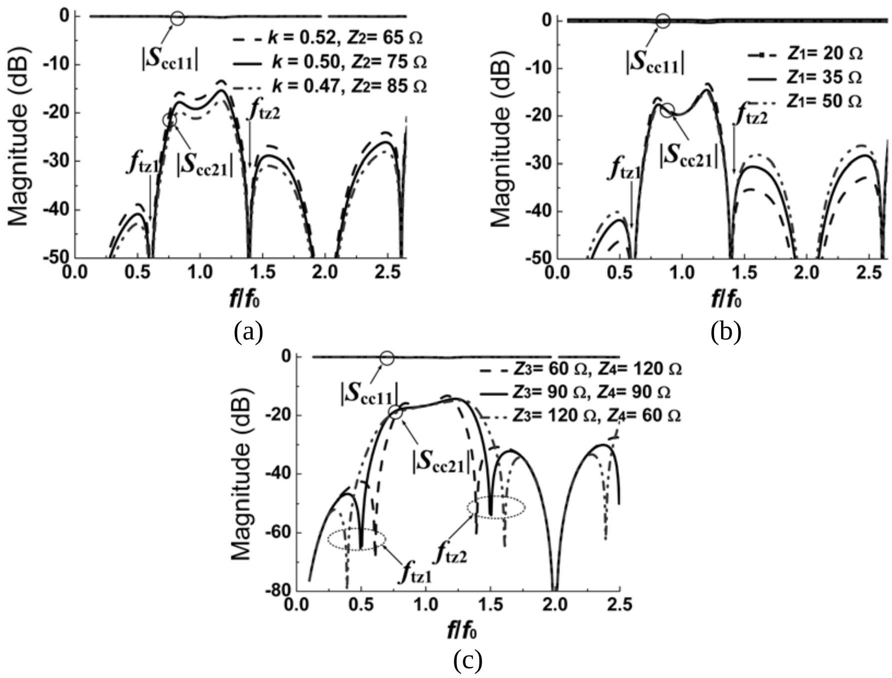

Figure 4. Simulated results of the common mode for the proposed wideband differential filter. (a) $|S_{cc21}|$ and $|S_{cc11}|$ versus Z_2 and k, $Z_1 = 30\,\Omega$, $Z_3 = 60\,\Omega$, $Z_4 = 120\,\Omega$. (b) $|S_{cc21}|$ and $|S_{cc11}|$ versus Z_1 and Z_4, $Z_1 = 30\,\Omega$, $Z_3 = 60\,\Omega$, $Z_4 = 120\,\Omega$, $Z_{oe} = 103.2\,\Omega$, $Z_{oo} = 63.2\,\Omega$. (c) $|S_{cc21}|$ and $|S_{cc11}|$ versus Z_3 and Z_4, $Z_1 = 30\,\Omega$, $Z_{oe} = 103.2\,\Omega$, $Z_{oo} = 63.2\,\Omega$.

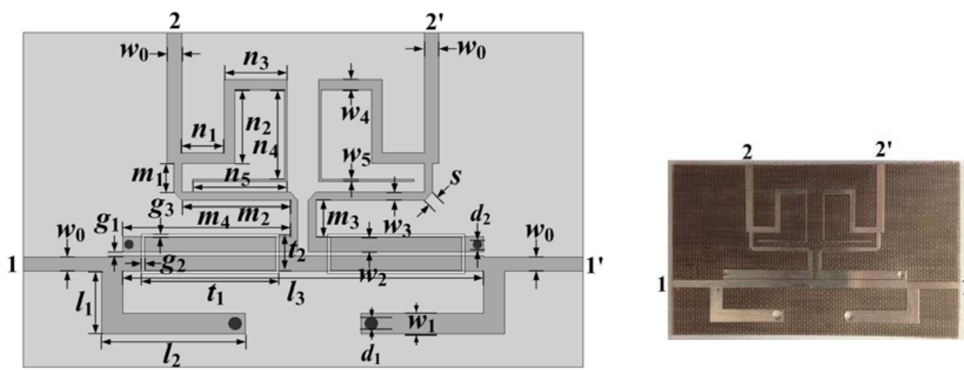

Figure 5. Top view and photograph of the wideband differential bandpass filter.

impedance resonators, transmission zeros located at f_{tz1} and f_{tz2} can be realized to improve the common mode suppression.

Based on the above theoretical analysis, the prototype of the proposed wideband differential filter structures with size of $50\,\text{mm} \times 30\,\text{mm}$ is shown in Figure 5, the final structure parameters for the wideband differential bandpass filter are: $l_1 = 6.3\,\text{mm}$, $l_2 = 13.6\,\text{mm}$, $l_3 = 34.2\,\text{mm}$, $m_1 = 2.75\,\text{mm}$, $m_2 = 10.25\,\text{mm}$, $m_3 = 3.5\,\text{mm}$, $m_4 = 15.85\,\text{mm}$, $n_1 = 4.0\,\text{mm}$, $n_2 = 7.0\,\text{mm}$, $n_3 = 6.0\,\text{mm}$, $n_4 = 8.5\,\text{mm}$, $n_5 = 9.0\,\text{mm}$, $t_1 = 13.0\,\text{mm}$, $t_2 = 3.8\,\text{mm}$, $w_0 = 1.4\,\text{mm}$, $w_1 = 2.3\,\text{mm}$, $w_2 = 1.62\,\text{mm}$, $w_3 = 0.75\,\text{mm}$, $w_4 = 1.0\,\text{mm}$, $w_5 = 0.24\,\text{mm}$, $g_1 = 0.15\,\text{mm}$, $g_2 = 0.3\,\text{mm}$, $g_3 = 0.3\,\text{mm}$, $s = 1.06\,\text{mm}$, $d_1 = 1.6\,\text{mm}$, $d_2 = 1.0\,\text{mm}$, $\varepsilon_r = 2.65$, $h = 0.5\,\text{mm}$, $\tan\delta = 0.003$. To realize the high impedance ratio of the shorted/open coupled line for single-layer PCB structure, patterned ground-plane technique proposed in [17] is used to solve the problem. For a simple microstrip coupler structure, the even-mode impedance is mainly relevant to the capacitance of the microstrip conductor to the ground plane, and the odd-mode impedance is related to the capacitance between the microstrip conductor and the ground plane, as well as the capacitance between the two coupled conductors [17]. With a slot under the coupled lines etched on the ground plane, the even- and odd-mode capacitances of the coupled lines would be decreased synchronously. However, the decrease of the even-mode capacitance is much faster than that of the odd-mode capacitance. In addition, the additional rectangular conductor etched on the ground is just located under the coupled lines and performs as one capacitor, therefore the odd-mode capacitance could be enhanced, and the high impedance ratio between the even- and odd-mode impedances for the coupled liens can thus be achieved [17]. The parameters of the coupled lines are given below, the width $W_2 = 1.62\,\text{mm}$, the gap $g_1 = 0.15\,\text{mm}$, and the original even- and odd-mode impedances of the coupled lines are $Z_{oe} = 52\,\Omega$, $Z_{oo} = 34.4\,\Omega$. After using the optimization procedure proposed in [17], the sizes of the slot in the ground to meet the impedances $Z_{oe} = 103.2\,\Omega$, $Z_{oo} = 33.2\,\Omega$ for the coupled lines are $g_2 = g_3 = 0.3\,\text{mm}$.

The design procedures of the wideband differential filter can be summarized as follows:

(1) Using the Equations (1)–(6), choose the desired bandwidth for the differential mode (greater than 50%) and the level of the common mode suppression ($|S_{cc21}| > 15\,\text{dB}$), determine the values of Z_{oe}, Z_{oo}, Z_1, Z_2, Z_3, and Z_4;

(2) When Z_1 and Z_2 are determined, use the commercial software in Ansoft Designer/ADS to determine the original values of Z_{oe}, Z_{oo}, and convert the even and odd-mode impedance to the physical dimensions of coupled-line with slotted ground plane using the proposed method in [16]; further optimize the values of Z_{oe}, Z_{oo}, Z_1, Z_2, Z_3, and Z_4, to realize better differential mode and common mode suppression transmission characteristics for the differential filter;

(3) Design proper layout and routing according to the connections and schematic simulation results; carry out full-wave electromagnetic simulation and dimension optimization for the differential mode and common mode transmission characteristics using a 3D EM simulator, such as Ansoft HFSS.

Based on the above theoretical analysis, the final parameters for the filter circuit of Figure 1(a) are given as follows: $Z_0 = 50\,\Omega$, $Z_1 = 30\,\Omega$, $Z_2 = 70\,\Omega$, $Z_3 = 60\,\Omega$, $Z_4 = 120\,\Omega$, $Z_{oe} = 103.2\,\Omega$, $Z_{oo} = 33.2\,\Omega$, $f = 3.0\,\text{GHz}$. The simulated results of the wideband differential bandpass filter are shown in Figures 6(a) and (b). For the differential mode, two transmission zeros are located at 1.85 GHz and 4.3 GHz with 3-dB bandwidth is 51.7% (2.2–3.75 GHz) and return loss greater than 10 dB (2.4–3.65 GHz); for the common mode, the $|S_{cc21}|$ is greater than 13 dB from 0 to 10.6 GHz ($3.5f_0$) and 10 dB from 0 GHz to 12.6 GHz ($4.2f_0$).

3. MEASURED RESULTS AND DISCUSSIONS

The prototype and photograph of the proposed wideband differential bandpass filter constructed on the dielectric substrate with $\varepsilon_r = 2.65$, $h = 0.5\,\text{mm}$, and $\tan\delta = 0.003$ is shown in Figure 5, and the measured and simulated results of the wideband differential bandpass filter are also shown in Figures 6(a) and (b). For the differential mode, the 3-dB bandwidth is 53% (2.26–3.85 GHz) with two transmission

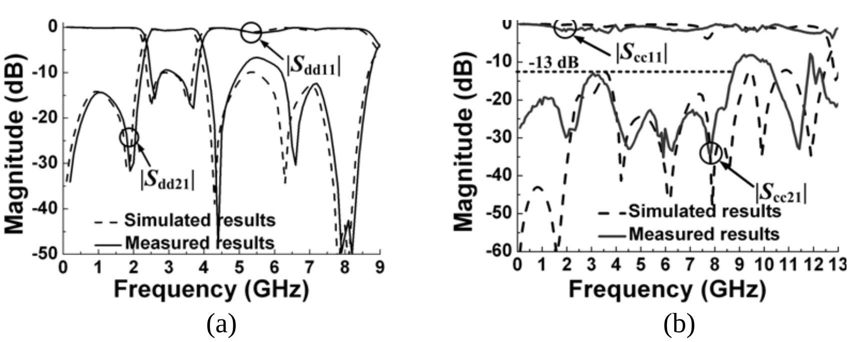

Figure 6. Measured and simulated results for the differential filter. (a) Differential mode. (b) Common mode.

Table 1. Comparisons of measured results for several wideband differential filter.

Filter Structures	Transmission zeros, $\lvert S_{dd21}\rvert$, 0–$2f_0$, (f_0)	3-dB bandwidth $\lvert S_{dd21}\rvert$	Core circuit size (λ_0^2)	$\lvert S_{cc21}\rvert$, dB (GHz)
Ref. [8]	4 (4.0 GHz)	62.5%	0.375	$>$ 20, (1.3–6.9)
Ref. [9]	4 (3.0 GHz)	79%	0.192	$>$ 13, (0–8.0)
Ref. [10]	2 (3.0 GHz)	110%	0.533	$>$ 15, (0–8.0)
Ref. [11]	3 (6.8 GHz)	75%	0.397	$>$ 15, (0–13.5)
Ref. [12]	2 (3.8 GHz)	105%	0.448	$>$ 40, (0–8.0)
Ref. [13]	2 (6.8 GHz)	111%	0.25	$>$ 13, (0–10)
Ref. [14]	4 (6.85 GHz)	70.7%	0.234	$>$ 13, (0–19)
Ref. [15]	2 (7.75 GHz)	38%	0.250	$>$ 15, (0–12)
This work	**4 (3.0 GHz)**	**53%**	**0.175**	**$>$ 13, 10 (0–9, 13)**

zeros located at 1.85 GHz and 4.3 GHz; for the common mode, over 13-dB stopband is obtained from 0 to 9.0 GHz ($3.0f_0$) and 10-dB from 0 GHz to 13 GHz ($4.3f_0$). The slight frequency discrepancies (less than 0.06 GHz) between the measured and simulated results are mainly caused by the limited fabrication precision and measurement errors.

To further demonstrate the performances of the wideband differential bandpass filter, the comparisons of measured results for several wideband differential filter structures [8–15] are shown in Table 1. Compared with the structures in [8–15], the core circuit size of the proposed wideband differential bandpass filter is only $0.175\lambda_0^2$, which is very compact. And wide stopbands for the common mode stretch up to $3f_0(\lvert S_{cc21}\rvert > 13\,\text{dB})$ and $4.3f_0(\lvert S_{cc21}\rvert > 10\,\text{dB})$.

4. CONCLUSIONS

A novel wideband differential bandpass filter using a Marchand balun with wideband common mode suppression is designed and analyzed. The bandwidth of the passband for the differential mode can be easily controlled by the even/odd-modes of open/shorted coupled lines. Two transmission zeros realized by two stepped impedance resonators are used to further improve the selectivity of the differential mode passband and common mode suppression. Good frequency selectivity and wideband common mode suppression can be realized for the wideband differential bandpass filter, indicating a good candidate for wideband balanced communication system.

ACKNOWLEDGMENT

This work is supported by the 2012 Distinguished Young Scientist awarded by the National Natural Science Foundation of China (61225001), Natural Science Foundation of Jiangsu Province (BK20140791) and the 2014 Zijin Intelligent Program of Nanjing University of Science and Technology.

REFERENCES

1. Eisenstant, W. R., B. Stengel, and B. M. Thompson, *Microwave Differential Circuit Design Using Mixed-mode S-parameters*, Artech House, Boston, MA, 2006.
2. Wu, C. H., C. H. Wang, and C. H. Chen, "Novel balanced coupled-line bandpass filters with common-mode noise suppression," *IEEE Trans. Microw. Theory Techn.*, Vol. 55, No. 2, 287–295, 2007.
3. Niu, J. X. and X. L. Zhou, "Analysis of balanced composite right/left handed structure based on different dimensions of complementary split ring resonators," *Progress In Electromagnetics Research*, Vol. 74, 341–351, 2007.

4. Shi, J. and Q. Xue, "Balanced bandpass filters using center-loaded half-wavelength resonators," *IEEE Trans. Microw. Theory Techn.*, Vol. 58, No. 4, 970–977, 2010.
5. Wu, S. M., C. T. Kuo, P. Y. Lyu, Y. L. Shen, and C. I. Chien, "Miniaturization design of full differential bandpass filter with coupled resonators using embedded passive device technology," *Progress In Electromagnetics Research Letters*, Vol. 121, 365–379, 2011.
6. Wu, S. M., C. T. Kuo, and C. H. Chen, "Very compact full differ-ential bandpass filter with transformer integrated using integrated passive device technology," *Progress In Electromagnetics Research Letters*, Vol. 113, 251–267, 2011.
7. Lim, S. C. and C. Y, Yeh, "Stopband-extended balanced filters using both $\lambda/4$ and $\lambda/2$ SIRs with common-mode suppression and improved passband selectivity," *Progress In Electromagnetics Research*, Vol. 128, 215–228, 2012.
8. Lim, T. B. and L. Zhu, "Highly selective differential-mode wideband bandpass filter for UWB application," *IEEE Microw. Wireless Compon. Lett.*, Vol. 21, 133–135, 2011.
9. Feng, W. J., W. Q. Che, Y. L. Ma, and Q. Xue, "Compact wideband differential bandpass filter using half-wavelength ring resonator," *IEEE Microw. Wireless Compon. Lett.*, Vol. 23, 81–83, 2013.
10. Wang, X. H., Q. Xue, and W. W. Choi, "A novel ultra-wideband differential filter based on double-sided parallel-strip line" *IEEE Microw. Wireless Compon. Lett.*, Vol. 20, 471–473, 2010.
11. Feng, W. J., W. Q. Che, T. F. Eibert, and Q. Xue, "Compact wideband differential bandpass filter based on the double-sided parallel-strip line and transversal signal-interaction concepts," *IET Microw. Antennas Propag.*, Vol. 6, No. 2, 186–195, 2012.
12. Lu, Y. J., S. Y. Chen, and P. Hsu, "A differential-mode wideband bandpass filter with enhanced common-mode suppression using slotline resonator," *IEEE Microw. Wireless Compon. Lett.*, Vol. 22, 503–505, 2012.
13. Zhu, H. T., W. J. Feng, W. Q. Che, and Q. Xue, "Ultra-wideband differential bandpass filter based on transversal signal-interference concept," *Electron. Lett.*, Vol. 47, No. 18, 1034–1035, 2011.
14. Feng, W. J. and W. Q. Che, "Novel wideband differential bandpass filter based on T-shaped structure," *IEEE Trans. Microw. Theory Techn.*, Vol. 60, 1560–1568, 2012.
15. Wang, H., W. Kang, G. Yang, and W. Wu, "A wideband differential bandpass filter based on T-shaped stubs and single ring resonator," *Progress In Electromagnetics Research Letter*, Vol. 40, 39–48, 2013.
16. Matthaei, G., L. Young, and E. M. T. Jones, *Microwave Filters, Impedance Matching Networks and Coupling Structures,* Artech House Inc., Norwood, MA, 1985.
17. Guo, Y. X., Z. Y. Zhang, and L. C. Ong, "Improved wide-band schiffman phase shifter," *IEEE Trans. Microw. Theory Techn.*, Vol. 54, No. 3, 2412–2418, 2006.